

We are IntechOpen, the world's leading publisher of Open Access books Built by scientists, for scientists

5,800

Open access books available

143,000

International authors and editors

180M

Downloads

Our authors are among the

154

Countries delivered to

TOP 1%

most cited scientists

12.2%

Contributors from top 500 universities



WEB OF SCIENCE™

Selection of our books indexed in the Book Citation Index
in Web of Science™ Core Collection (BKCI)

Interested in publishing with us?
Contact book.department@intechopen.com

Numbers displayed above are based on latest data collected.
For more information visit www.intechopen.com



Chapter

Perspective Chapter: Interpretation of Deep Foundation Load Test Data

Jon Sinnreich

Abstract

Static load tests are seen by many practitioners as the best techniques to approximate in-service conditions for deep foundation elements and to validate analytical model predictions of capacity and settlement. Full-scale static load tests are fairly expensive to implement, especially as part of a pre-construction investigation when equipment and personnel must be mobilized to site separately to specifically install the test element(s). Test elements are often instrumented with strain gages to determine the load distribution during the test. Correct installation of gages and interpretation of the resulting data is critical to properly evaluate the test results and recoup the significant investment made in conducting the test. This paper discusses several key points in the interpretation of strain gage data in deep foundation load tests.

Keywords: strain gages, deep foundation load testing, tangent stiffness, incremental rigidity, t-z curves

1. Introduction

Static load tests are seen by many practitioners as the premier techniques to approximate in-service conditions for deep foundation elements and to validate analytical model predictions for load-bearing capacity and settlement. Full-scale static load tests are fairly expensive to implement, especially as part of a pre-construction investigation when equipment and personnel must be mobilized to site separately to specifically install the test element(s). Test elements are often instrumented with strain gages to determine the load distribution during the test. Correct installation of gages and interpretation of strain data is critical to properly evaluate the test results and recoup the significant investment made in conducting the test.

The ultimate product of a foundation test strain data analysis is often a set of curves which model the non-linear unit soil response to shear and bearing load (typically called 't-z' and 'q-z' curves, respectively). These curves are useful to model the foundation response to load [1]. Strain gage data is utilized to compute both the shear and bearing ('t') and displacement ('z') portions of the curves.

In the first section, statistical results collected by the author in two large-scale test programs involving multiple test foundations each are analyzed to investigate the optimal positioning of strain gages in a test element. In the second section, the

conversion of strain to force via the rigidity function is discussed. In the third section, use of strain data to properly calculate zone displacement is derived.

2. Optimal strain gage arrangement

The discussion in this section was originally published in [2]. The assumption of axial plane-strain is significant to converting measured strain to axial force. Eccentric stress in the foundation element whether due to inclined or eccentric loading, uneven soil resistance, irregular foundation cross-section shape or other reasons will cause an uneven distribution of strain across the element cross-section. Based on Euler beam theory, the total strain is a superposition of axial strain (which is required to compute axial load) and bending strain which is disregarded. In axial compressive or tensile load testing of foundations it is presumed that axial strains due to applied loading will be significantly greater than incidental bending strains due to load eccentricity or other second-order causes. Total strain is assumed to be linearly distributed across the plane of the element, and the net average axial strain will intersect the centroid of the element. Therefore, obtaining the strain at the centroid is key to computing the net axial force.

The theoretical performance of gages arranged in various configurations and then averaged for the purpose of force calculation is validated using statistical results collected during the course of two large-scale test programs (the 'Florida' case history and the 'California/Nevada' case history, respectively), each involving multiple test foundations.

Normally, two or more strain gages are installed in a test foundation per level, attached to the steel reinforcement. Spacing the gages symmetrically around the perimeter allows for an estimate of the strain at the centroid to be computed as an average of the individual strain measurements. One opposed pair of gages is the typical arrangement. In the Florida case history test program, the owner specified three gages per level. It was not explicitly stated, but the implied arrangement was an equal spacing of 120° around the perimeter of the pile reinforcement cage (Figure 1).

Strain gages installed in cast-in-place foundation elements the field have a percentage mortality rate (probability of failure), designated λ . This is most often due to installation procedures for deep foundations. When constructing drilled shafts,

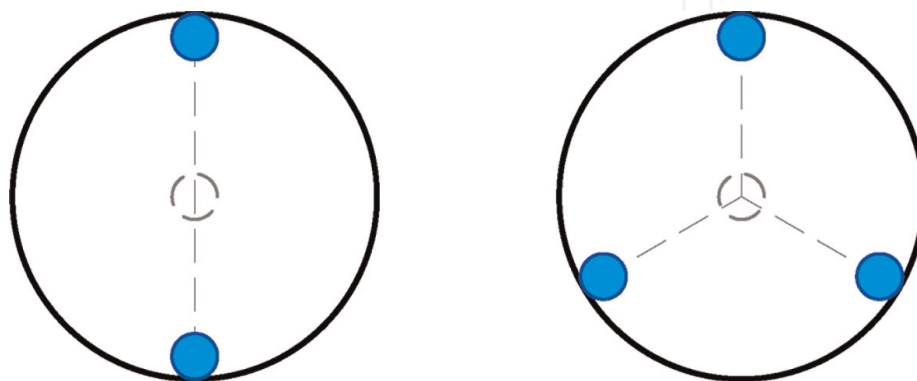


Figure 1. Typical arrangement of opposed pair and triplet strain gages in pile cross section with computed average (dashed lines).

reinforcement cages must be lifted by crane, rotated from horizontal to vertical and then inserted into the shaft excavation. Concreting then takes place, either via the tremie method or by gravity pour, both of which are dynamic procedures with many opportunities to damage a gage. For auger-cast-in-place (ACIP) piles, the relatively slender and flexible reinforcement cage is lifted into the air at the head only for rapid insertion into fluid grout, which induces a 90° bend into the cage as it is lifted. In the Florida case history testing program, from a total of 657 sisterbar vibrating wire strain gages installed in eleven bi-directional ACIP test piles, seventeen gages failed to function during testing, yielding a mortality rate λ of 2.6%.

To estimate the strain at the centroid of the foundation element, the symmetrically-arranged gages at a given level are averaged. All the gages at a given level must function in order to compute the average at the centroid. Given k gages at a level, the probability of success S in this situation is computed as the simultaneous probability of survival of all the gages:

$$S_k = (1 - \lambda)^k \quad (1)$$

Even though in practice if a single gage fails the remaining gage(s) are often still utilized to estimate the average strain, this is not optimal since the resulting average is now off the centroid and therefore may not be representative of the average axial load if an uneven strain distribution is present in the cross-section due to bending stress.

To evaluate the potential significance of the difference between using an opposed-pair average and a single gage (assuming its opposite malfunctioned), data from a total of 207 pairs of functioning opposed gage pairs in the eleven axial test piles in the Florida case history is analyzed. A relative difference is computed for each logged reading of each opposed gage pair:

$$d = \frac{|\varepsilon_1 - \varepsilon_{avg}|}{\varepsilon_{avg}} \quad \text{where } \varepsilon_{avg} = \frac{\varepsilon_1 + \varepsilon_2}{2} \quad (2)$$

For each gage pair, the differences are averaged for all increments of loading. The resulting 207 data points are plotted on a histogram, and a log-normal probability distribution function is fitted to the resulting data (**Figure 2**).

The results of this analysis indicate that for this data set, the mean difference between data from a single gage and the average of the opposed pair is 15.3%, a significant dissimilarity. The inset figure plots the difference between individual and averaged strains as a percentage versus maximum average strain, which ranged from single digits of microstrain in gage levels near the ground surface to over 1000 microstrain in the vicinity of the bi-directional jacks. Although several of the highest individual difference values correspond to the smallest maximum strains, there is a fairly even distribution and no strong correlation to absolute values of strain, indicating the high mean difference is not confined to gage levels recording relatively little total strain (in other words, due essentially to a low signal-to-noise ratio). Obtaining a good measure of the average strain, rather than relying on an off-center result is thus crucial to computing the correct axial force.

Using Eq. (1), the surprising conclusion is reached that installing three equally-spaced gages per level (presumably for additional redundancy) actually results in a lower probability of successfully in obtaining the average strain at the pile centroid (92.4%) than by using two gages in an opposed pair (94.9%, using the numeric

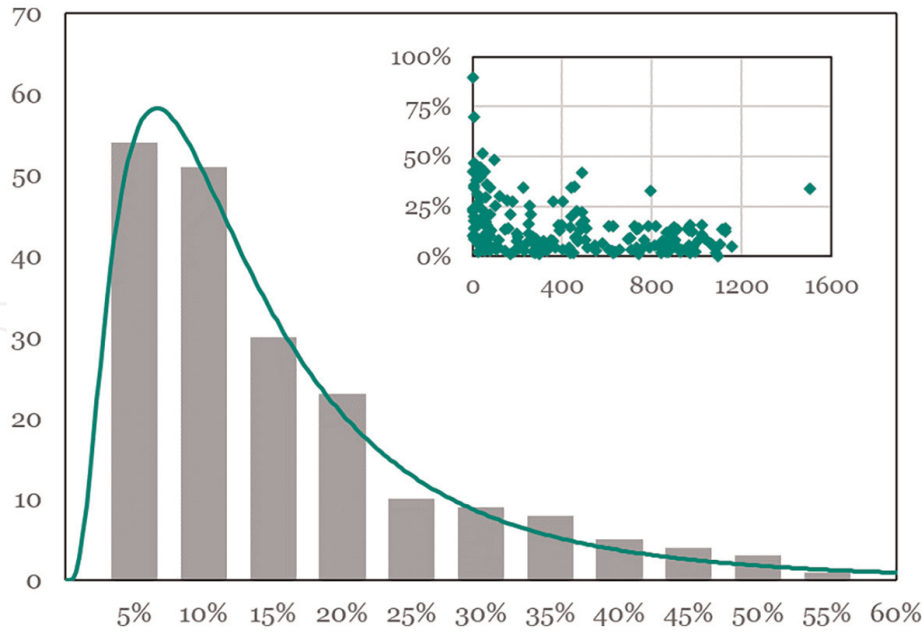


Figure 2. Histogram and estimated probability distribution for percent difference between individual and averaged strains (inset figure – Percent difference vs. maximum average strain).

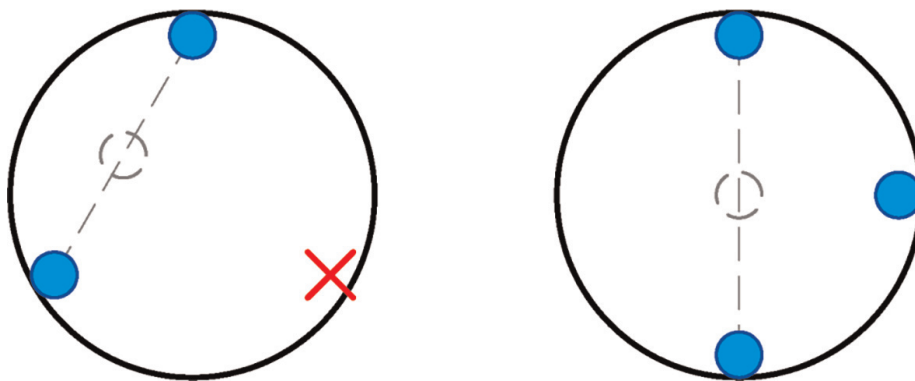


Figure 3. Strain gage triplet averaging results with defective gage (left), and with 0°, 90°, 180° arrangement (right).

values for this case history). This is because in either arrangement, the average strain at the centroid is successfully computed only if all the gages function, and assuming each individual gage has an equal probability of malfunction, there is a higher cumulative probability of losing one gage out of three installed than one out of two installed.

In this test program the three specified gages were installed at 0°, 90° and 180° around the rebar cage at each level (see **Figure 3**). The gage at the 90° position was logged but the data was not used in the analysis of results unless one of the other gages malfunctioned. This resulted in a slight improvement in the overall test program; five of the seventeen malfunctioning gages were at the 90° position, resulting in no negative effect on the data analysis.

Substantial redundancy is achieved by installing four strain gages per level, if they are viewed as two independent sets of opposed pairs. If all four gages function properly, then the average strain is computed from all four. However, if any one gage malfunctions, it and its opposed twin is discarded and the average is computed from the remaining opposed pair only, which should still yield a good measure of strain at

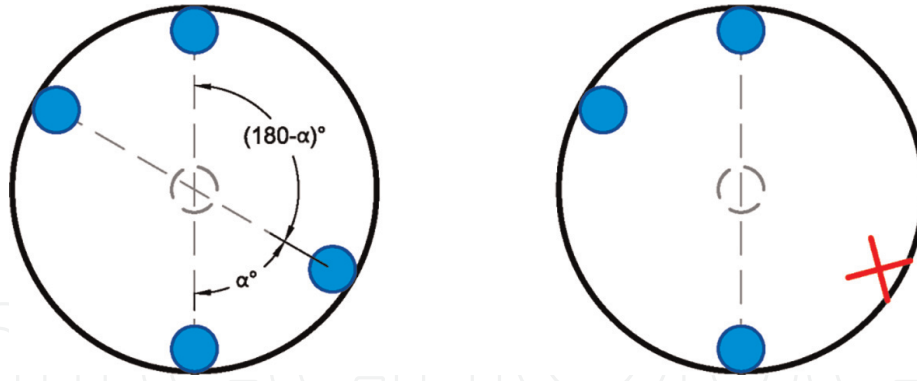


Figure 4.
 Averaging results for two opposed pairs of strain gages.

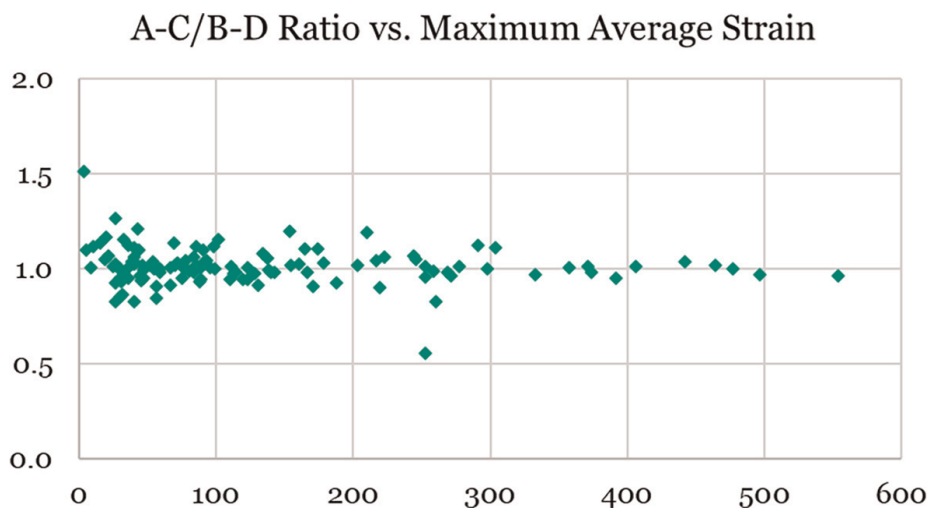


Figure 5.
 Scatterplot of ratio of maximum A-C average to B-D average versus overall maximum strain.

the pile centroid. Note that the gages do not have to be spaced at 90° angularly; each pair needs only to be 180° opposed (**Figure 4**).

The probability of success $S_{2 \times 2}$ for this arrangement is computed as one minus the probability of simultaneous failure of both opposed pairs:

$$S_{2 \times 2} = 1 - (1 - S_2)^2 = 1 - (1 - (1 - \lambda)^2)^2 \quad (3)$$

For the Florida case history, using the same value λ of 2.6% results in a probability of success of 99.7% (up from 94.9% using two gages in a single opposed pair).

The California/Nevada case history data set consisted of a total of 488 gages in 122 functioning quartets from sixteen drilled shaft tests. By convention, the gages are designated A, B C and D, clockwise in plan around the rebar cage perimeter. The two opposed pairs are then labeled A-C and B-D, respectively. **Figure 5** plots the ratio of the maximum average strain of the A-C pair to the B-D pair versus the average of all four gages.

The average of the ratios is 1.01, indicating that in general the A-C and B-D pairs converge on the same average strain value. However, the standard deviation is 0.10, meaning on average there is a potential for approximately 10% deviation in the

measured strain (and thus computed load) using one versus two pairs of gages. Depending on the test objectives, this value may be significant enough to justify specifying four gages per level.

The purpose of embedding strain gages in a test foundation is to determine the load distribution (see below) and from it, the t - z and q - z curves. As such, there are two possible strategies to consider when deciding on the location (depth in the foundation) for each level of strain gages. The first approach will seek to identify the shear capacity of distinct soil layers in the stratigraphy. Based on a nearby (or ideally, centerline) soil boring, gages should be positioned at the interfaces between various soil strata to separately identify the capacity of each. Alternatively, if the test data is to be used as input to a finite-difference computer model such as FB-MultiPier, the gages should be positioned at an even spacing corresponding to the node spacing in the computer model. Consultation with the design engineer during the planning phase of a load test program will help identify test objectives and inform the optimal layout of strain gage levels. As a general guideline, gages should not be located closer than one element diameter to boundaries of the foundation (top, base and/or embedded loading device for bi-directional tests), in order to assure a plane-strain condition.

3. Incremental back-calculation

The function which converts axial strain to stress in a deep foundation is the multiplier consisting of Young's modulus of the foundation material E times the cross-sectional area A . This function is often called the 'stiffness' of the foundation, although technically this is a misnomer since by definition the units of stiffness are force per length (AE/L), whereas the conversion of strain (unitless) to force must also be defined in units of force (AE), and is properly called the 'rigidity.' Composite axial rigidity calculations based on empirical relationships such as the ACI 318 formula [3] result in a constant value of AE . These types of empirical formulas are based on several assumptions, including average concrete strength f'_c and knowledge of the cross-sectional area, which may be only nominally correct. In addition, confinement effects and the fact that the stress-strain relationship (modulus) of cementitious materials is not linear are also not considered.

The basic assumption of incremental rigidity back-calculation methods is that the non-linear stress-strain relationship of cementitious materials (drilled shaft concrete and augercast pile grout) can be adequately approximated with a quadratic function [4]. This assumption seems reasonable if a family of stress-strain curves is examined (Figure 6), with a parabola (red-dashed line in the figure) overlaid over the $f'_c = 4000$ psi curve as an illustrative example. The approximation is quite good from the origin up to the peak stress (yield point), which is all that is required for the analysis of load test results. The value of Young's modulus is the slope of the stress-strain function curve at any given strain. As noted in the case histories in the previous section, it is not uncommon during axial load testing to measure strains on the order of 500 to 1000 $\mu\epsilon$ or more, especially in slender elements such as ACIP piles. Therefore, the non-linearity of Young's modulus of cementitious materials must be accounted for.

The axial rigidity contribution of steel reinforcement in the composite cross-section is typically relatively small, and the stress-strain curve for steel is assumed linear up to the yield point which means its modulus is relatively constant. Therefore,

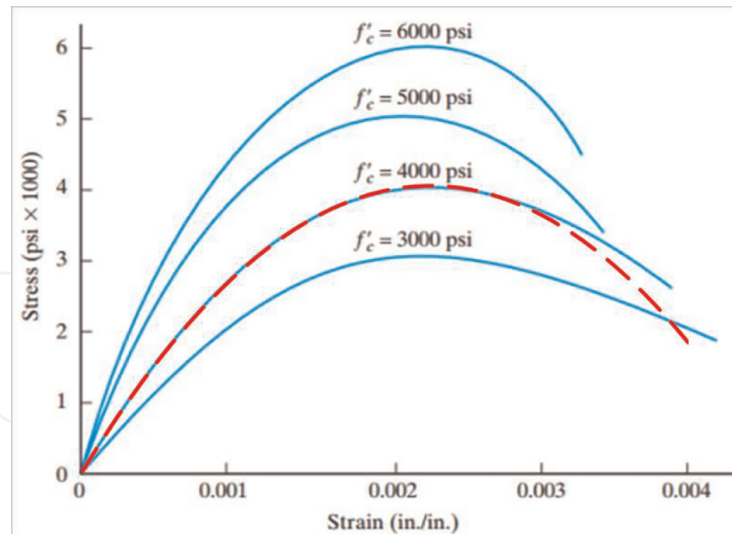


Figure 6.
 Concrete stress-strain curves and quadratic approximation (red dashed line).

the non-linear properties of the cementitious material govern the composite cross-section rigidity of the foundation element.

The equation of the parabolic quadratic function illustrated in **Figure 6** is given by:

$$\sigma = a\varepsilon^2 + b\varepsilon + c \quad (4)$$

Note the constant term c is always zero, which assures that the parabola intersects the origin. The cross-sectional area is assumed to remain constant throughout the analysis; the small effect of Poisson's ratio is neglected. Therefore, to convert from stress to force and modulus to rigidity, Eq. (4) is simply scaled by the cross-sectional area A :

$$F = A\sigma = A(a\varepsilon^2 + b\varepsilon) \quad (5)$$

3.1 Incremental back-calculation

The Secant Modulus (SM) method is the simplest back-calculation technique. A strain gage (or set of strain gages) is installed in the deep foundation element at or above ground level, such that all of the applied force P at the head of the element must be registered by the gage(s). That is to say, no force is shed into the soil via skin friction between the point of load application and the strain measurement. At each incremental step n of the load test, the rigidity is computed as:

$$(AE_n)_{secant} = \frac{P_n}{\varepsilon_n} \quad (6)$$

Note that the method is typically discussed in terms of stress and strain [5, 6]. Starting with test load data, the foundation cross-sectional area is divided out in order to derive a function for the modulus. In order to recover forces, the cross-sectional area must be multiplied back into the analysis later. Herein, this intermediate step is eliminated since the ultimate objective is to convert strain data to force.

This method is called ‘secant’ because the resulting rigidity function is the slope from any point on the force-strain curve back to the origin. Once testing is complete, each of the rigidity values AE_n are plotted versus ε_n , and linear regression is used to determine the slope and offset (a and b respectively) of the best-fit line through the data. Substituting Eq. (5) into Eq. (6), the result in terms of the quadratic function presented above is:

$$(AE)_{secant} \approx \frac{F}{\varepsilon} = \frac{A(a\varepsilon^2 + b\varepsilon)}{\varepsilon} = A(a\varepsilon + b) \quad (7)$$

To compute the force at any strain, Eq. (7) is rearranged:

$$F_n = A(a\varepsilon_n^2 + b\varepsilon_n) \quad (8)$$

One drawback of this method is that it cannot be utilized during bi-directional testing. The plane-strain assumption (the strain measured by the gages is an accurate representation of the average strain throughout the cross-section) means that the gages must be positioned at least one element diameter away from the point of loading, in order for local stress variations at the point of loading to even out. In a bi-directional test, significant force may be shed into the soil via skin friction within this span, invalidating the relationship in Eq. (6) because the force at the strain gage location is now an unknown.

Additionally, in cast-in-place foundation elements (with variable cross-section area and curing conditions), or those which have variable reinforcement with depth, the SM method may not yield accurate rigidity estimates for embedded strain gage levels because the ground-level gages may not be representative [7].

3.2 Tangent modulus and incremental rigidity methods

The Tangent Modulus (TM) method was initially derived by Fellenius explicitly for the modulus, with the cross-sectional area considered separately. This is best applicable for foundation elements with assured constant cross-section properties (such as driven piles). The Incremental Rigidity (IR) method discussed in [7, 8] recognized that the rigidity (modulus times area, AE) is a single function which can be identified without explicitly identifying the relative magnitude of either of the two components A and E . In this discussion the analysis focuses on the strain-force relationship (effectively, the Incremental Rigidity method), although from a strictly mathematical derivation standpoint, the TM and IR methods are equivalent.

In the IR method, rigidity is computed as the slope of the force-strain curve at a given strain. This slope is approximated as the change in applied load ΔP divided by change in strain $\Delta\varepsilon$ for successive load increments:

$$(AE_n)_{incremental} \approx \frac{\Delta P}{\Delta\varepsilon} = \frac{P_n - P_{n-1}}{\varepsilon_n - \varepsilon_{n-1}} \quad (9)$$

As with the SM method above, once testing is complete the rigidity value at each increment is plotted against its corresponding strain and a best-fit line plotted through the data. However, the incremental method requires that the side shear section between the point of load application and the strain gage elevation has reached or at least approached its ultimate capacity. Because of shear resistance, the force increase

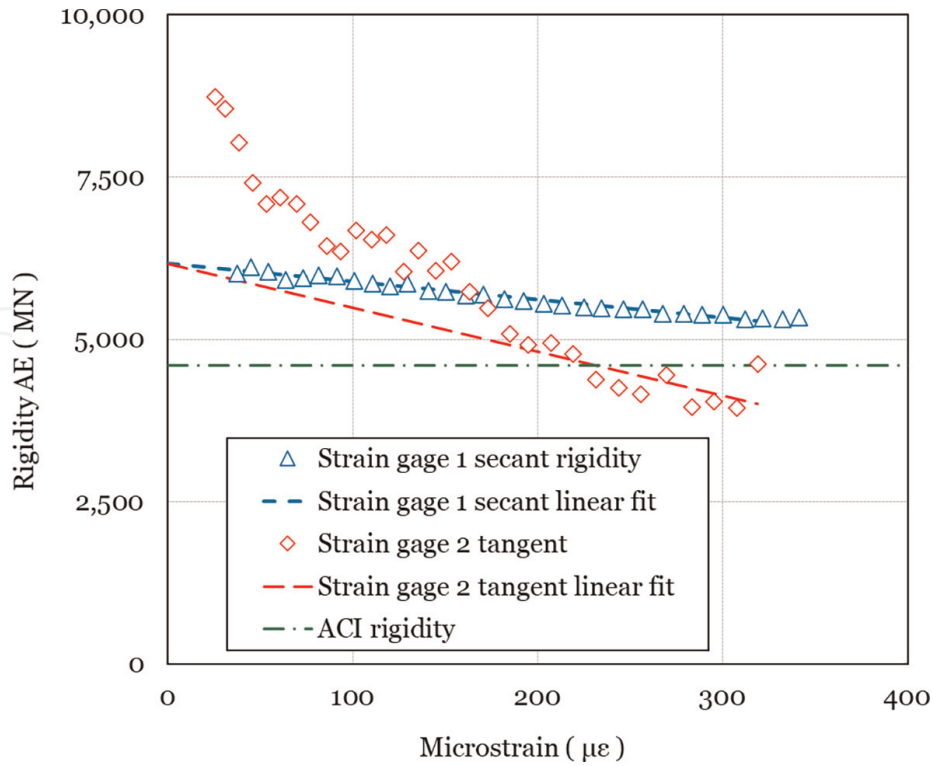


Figure 7.
 Sample rigidity analysis from strain gage data.

at the strain gage will be less than the applied load increase during the initial part of the test. Therefore, the resulting incremental rigidity values will be excessive. It is only after the side shear section between the point of load application and the strain gage reaches its ultimate shear capacity that subsequent applied load increments result in strain increments which give a true indication of the rigidity. This behavior becomes apparent on a plot of the analysis where the rigidity decreases from very high values at a small ϵ to a linear curve at high ϵ (see **Figure 7**, above). A linear regression through this ultimate portion of the incremental rigidity curve will yield slope and offset values g and h :

$$(AE)_{incremental} = A(g\epsilon + h) \quad (10)$$

The incremental rigidity, by definition is also the slope (first derivative) of the force-strain function (Eq. (5)):

$$(AE)_{incremental} = dF/d\epsilon = A(2a\epsilon + b) \quad (11)$$

Comparing Eqs. (7), (8) and (11) it becomes apparent that the incremental rigidity and secant rigidity analyses for the same load test will result in a different force-strain relationship, by a factor of 2 in the first term (slope) and that the second term constants (b and h respectively) are equivalent. This is illustrated in **Figure 7** with a sample data set from a series of top-down tests (the ‘Texas’ case history). Strain gage 1 is located just below the point of load application, and is analyzed using the secant rigidity method. Strain gage 2 is located some distance down within the shear embedment zone, and is analyzed using the incremental rigidity method. As expected from theory, the two linear regressions converge at the vertical axis (the zero-strain condition) but have significantly different slopes. For comparison purposes, the ACI

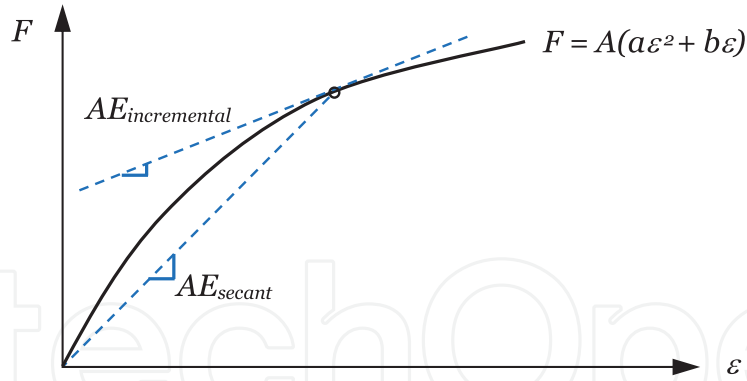


Figure 8. Non-linear force-strain curve with incremental (tangent) and secant moduli.

rigidity (computed using the empirical relationship to the square root of concrete strength f^c) is also plotted as a horizontal line, showing that it does not produce a good result for this particular foundation element.

Because it is the slope from any point on the force-strain curve back to the origin, the secant rigidity can be multiplied by any measured strain to directly compute force. However, the incremental rigidity cannot be simply multiplied because it is by definition tangent to the force-strain curve at all points and does not intercept the origin. **Figure 8** illustrates this point graphically.

By simply multiplying the curve-fit incremental rigidity slope by 0.5, the equivalent secant rigidity function is recovered and Eq. (12) used to compute the force directly for each measured strain.

$$F_n = A(0.5(g\varepsilon_n^2) + h\varepsilon_n) = A(a\varepsilon_n^2 + b\varepsilon_n) \quad (12)$$

Alternatively, or when dealing with highly non-linear rigidity relationships, the value of F at any loading point n may be approximated by a recursive summation formula [9]:

$$F_n = F_{n-1} + (AE_n)_{incremental}(\varepsilon_n - \varepsilon_{n-1}) \quad (13)$$

where F_{n-1} and ε_{n-1} are the force and strain of the previous loading data point, respectively. This step-wise approximation will roughly follow the curved load-strain path.

This approach will give approximately correct results even if the rigidity function is highly non-linear, such as in the case of a tensile load test once the cementitious material begins to crack due to tensile strain, or in a compressive load test with pre-existing tension cracks in the cementitious material which are closed up by the compressive axial stress [9]. As noted above, foundation element axial rigidity AE is composed of two contributors, steel and cementitious material (A_sE_s and A_cE_c , respectively). For a cementitious material which is fractured (due to shrinkage during curing or applied tensile stress), the nominal area A_c is replaced with an effective area A'_c .

Figure 9 illustrates two idealized functions of nonlinear axial rigidity due to cementitious material fracturing in response to tensile stress (bold line segments). The full composite rigidity consists of $A_sE_s + A_cE_c$. The angular pathways to/from the reinforcing steel rigidity (A_sE_s only) indicate idealized changes in rigidity due to fracturing with increasing strain. With increased compressive strain pre-existing

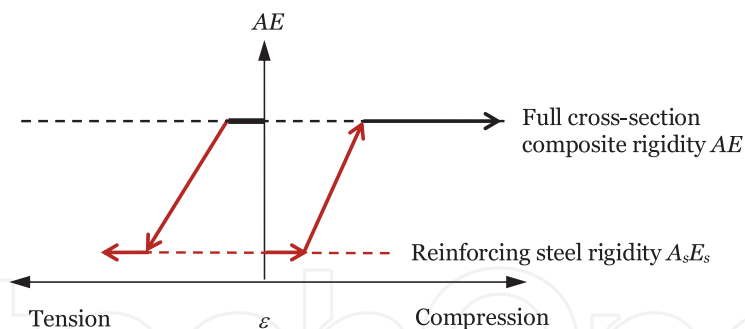


Figure 9.
Possible non-linear rigidity function paths.

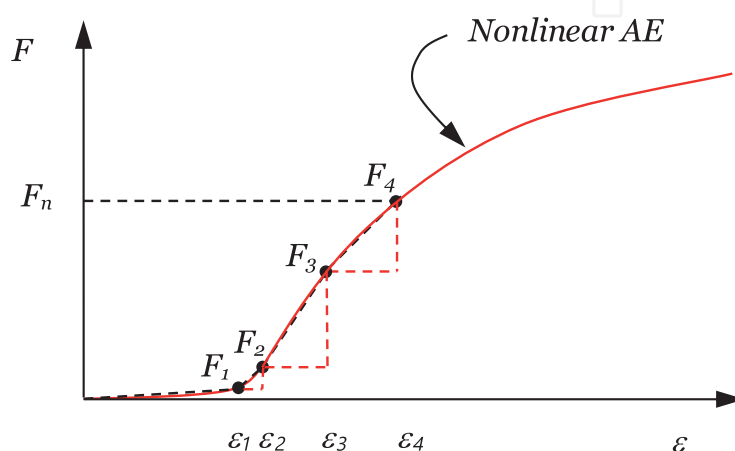


Figure 10.
Incremental load calculation.

fractures progressively close up, A'_c increases from zero to A_c and the rigidity increases until the full composite rigidity is reached. Conversely, with increased tensile strain, the rigidity decreases from the full composite value down to the reinforcing steel rigidity only, as the cementitious material progressively fractures until only the reinforcing steel remains to transmit stress.

If Eq. (13) is employed, using each load test increment as a discrete step the non-linear load-strain curve can be approximated by a series of small incremental increases in load, each of which is linear with its corresponding increase in strain, as illustrated in **Figure 10**.

Note that all the rigidity back-calculation methods depend on obtaining high-quality strain gage data from relatively small, equal load increments to clearly define trends. Results obtained at one strain gage level may not apply at other levels, due to several factors including possible changes cross-sectional area, reinforcement details, confinement (within rock socket as opposed to overburden) and differing concrete curing conditions (hydrostatic pressure, water table elevation, environmental temperatures, etc.) among others.

Once the load at each strain gage level has been computed using the methods discussed above at every load increment, a family of load distribution curves can be generated (see **Figure 11**).

The difference between adjacent levels (a 'zone' of the foundation element), divided by the perimeter shear area of the zone, gives the unit shear, the 't' component of the desired t-z curve. A level of strain gages placed near the base of the foundation also allows for estimation of the bearing resistance q .

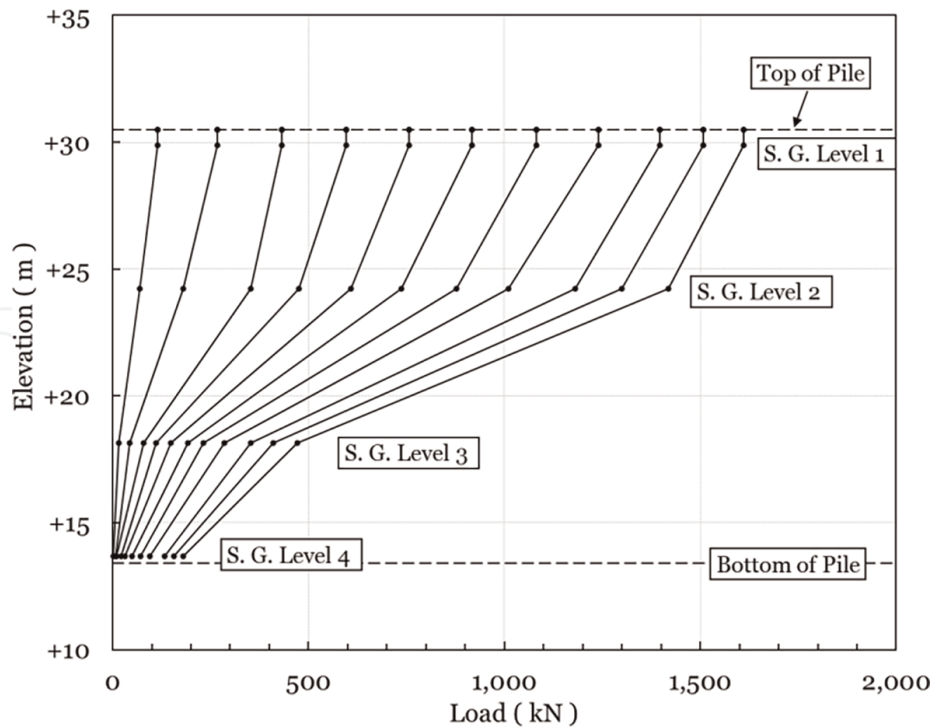


Figure 11.
Sample load distribution (Texas case history).

Note that the analysis results presented herein are based on re-zeroing all strain gages prior to the start of loading, and account for the resistance of the as-built isolated test element to a relatively short-duration externally-applied load only. They do not account for any residual load present in the element at the start of testing, down-drag, long-term setup, creep or group effects.

4. Compression and displacement

To a first-order approximation, the displacement of each zone of an axially-loaded deep foundation is the measurement D given by dial gages or displacement transducers at the head, or point of load application in bi-directional load tests. However, as discussed above the foundation element has a rigidity, which means it will compress or elongate elastically under applied stress. The degree of this compression or elongation can be estimated using the collected strain gage data.

For each zone, the zone strain is computed as the average of the measured strains at the top and bottom of the zone. Change in length (compression or elongation) δ is then computed as the average zone strain times the zone length L .

$$\epsilon_{zone} = \frac{\epsilon_{top} + \epsilon_{bottom}}{2}, \delta_{zone} = \epsilon_{zone} \cdot L_{zone} \quad (14)$$

Zones which do not have strain gage levels both at the top and bottom, but rather are located next to boundary changes (the zone(s) adjacent to the load-application device and/or the top and bottom of the foundation element) must be evaluated differently. Depending on the situation, the one available strain gage level may be assumed to be representative of strain throughout the zone, strain data from two or

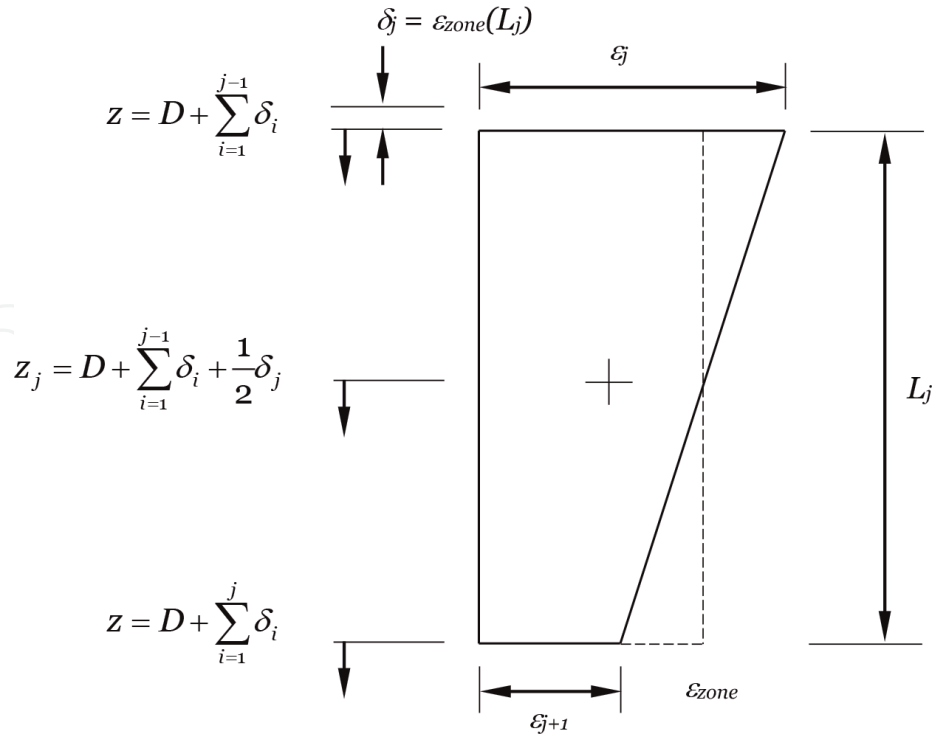


Figure 12.
 Calculation of average strain, compression and displacement at top, mid-point and bottom of a zone.

more levels may be extrapolated, or strain may be estimated by correlation to extensometer telltale rod data.

The total displacement of each zone z_j is then computed at the midpoint of the zone. The calculation must include the displacement at the point of load application D as well as the change in length of all zones between the point of load application and the current zone:

$$z_j = D + \sum_{i=1}^{j-1} \delta_i + \frac{1}{2} \delta_j \quad (15)$$

This calculation will then result in the 'z' component of the t-z curve for every shear zone. **Figure 12** is a schematic of the zone displacement calculation.

In certain circumstances, the elastic compression of the test foundation may be a minor contributor to the total computed displacement. However, in situations with very stiff soils or rock, and/or with slender elements with a relatively small rigidity and large strains, the elastic deformation can be a significant if not major portion of the total displacement of each shear zone. While the interpretation of data described in this section is simpler than in the previous sections, it is no less critical to constructing the t-z and q-z curves from strain data correctly.

5. Conclusions

Strain gages are critically important instruments for monitoring the performance of a deep foundation element undergoing a load test. Strain gage data must be properly analyzed in order to gain insight into the true soil-structure interaction. In order


to verify design assumptions and particularly to optimize computer models, the unit capacity curves (so-called t-z and q-z curves) must be obtained from the load test. Properly analyzed strain gage data contributes to both components of these curves. However, strain gages are not load cells – the conversion of strain to load is not as straightforward as linear elastic theory may lead one to believe. Careful attention must be given to the selection, placement, monitoring and interpretation of strain gages in deep foundation load testing. The techniques described herein have been developed and successfully deployed by the author and others for over two decades to utilize strain gages in deep foundation load testing.

Author details

Jon Sinnreich
Load Test Consulting Ltd., Gainesville, FL, USA

*Address all correspondence to: jon@ltc-us.com

IntechOpen

© 2022 The Author(s). Licensee IntechOpen. This chapter is distributed under the terms of the Creative Commons Attribution License (<http://creativecommons.org/licenses/by/3.0>), which permits unrestricted use, distribution, and reproduction in any medium, provided the original work is properly cited. 

References

- [1] Meyer PL, Holmquist DV, Matlock H. Computer predictions for axially-loaded piles with non-linear supports. In: 7th Offshore Technology Conference. Houston, TX: American Petroleum Institute; 1975. pp. 375-387
- [2] Sinnreich J. Optimizing the arrangement of strain gauges in pile load testing. ASTM GTJ. 2020;44(5): 1552-1558. DOI: 10.1520/GTJ20200033
- [3] ACI. Building Code Requirements for Structural Concrete (ACI 318–14) and Commentary. American Concrete Institute. Michigan, USA: ACI World Headquarters: Farmington Hills. 2014
- [4] Sinnreich J. A discussion of Back-calculated rigidity methods. In: DFI SuperPile '22. St. Louis, MO: Deep Foundation Institute; 2022
- [5] Fellenius BH. Tangent modulus of piles determined from strain data. In: ASCE Geotechnical Division 1989 Foundation Congress. Vol. 1. Evanston IL: American Society of Civil Engineering; 1989. pp. 500-510
- [6] Fellenius BH. From strain measurements to load in an instrumented pile. Geotechnical News. 2001;19(1):35-38
- [7] Komurka VE, Robertson S. Results and lessons learned from converting strain to internal force in instrumented static loading tests using the incremental rigidity method. In: ASCE Geo-Congress 2020. Minneapolis MN: American Society of Civil Engineering; 2020. pp. 135-152
- [8] Komurka VE, Moghaddam RB. The incremental rigidity method – More-direct conversion of strain to internal force in an instrumented static loading test. In: ASCE Geo-Congress 2020. Minneapolis MN: American Society of Civil Engineering; 2020. pp. 124-134
- [9] Sinnreich J. Strain gage analysis for nonlinear pile stiffness. ASTM GTJ. 2012;35(2):367-374. DOI: 10.1520/GTJ103412